GMR
The Original

GREEN AND CHEMICAL SYNTHESIS OF A-FE_2O_3 NANOPARTICLES: STRUCTURAL, MORPHOLOGICAL AND ELEMENTAL CHARACTERIZATION

[1]Dipak Sonawane, [2]Ashwini Kanade, [3]Naziya M.A. Rehman, [4*]Kalpana G. Joshi

[1]Department of Interdisciplinary Studies, School of Interdisciplinary Studies, Sanjivani University, Kopargaon, Maharashtra, India, Email: de.sonawane85@gmail.com
[2]Department of Chemistry, School of Science, Sandip University, Nashik, Maharashtra, India, Email: ashwinisonawane89876@gmail.com
[3]Dr.BAMU, Chht. Sambhaji Nagar, Maharashtra, India, Email: nazirehman786@gmail.com
[4*]Department of Interdisciplinary Studies, School of Interdisciplinary Studies, Sanjivani University, Kopargaon, Maharashtra, India, Email:kalpanajoshiset@sanjivani.edu.in

ABSTRACT:
Environmental contamination by toxic heavy metals poses a serious threat to ecosystems and human health, necessitating the development of efficient, eco-friendly remediation materials. In the present study, iron oxide nanoparticles were synthesized using two approaches: a conventional chemical route and a green synthesis method employing Spondias dulcis leaf extract as a natural reducing and stabilizing agent. The synthesis process was monitored through visual and reaction-based observations, where a progressive color transition from pale yellow to dark brown and finally black confirmed nanoparticle formation, followed by magnetic separation and purification. The synthesized nanoparticles were characterized using X-ray Diffraction (XRD), Scanning Electron Microscopy (SEM), and Energy Dispersive X-ray Spectroscopy (EDX). XRD analysis revealed sharp and intense diffraction peaks, confirming crystalline structure and successful formation of iron oxide nanoparticles. SEM analysis demonstrated nanoscale spherical to quasi-spherical morphology with varying degrees of aggregation, while EDX and elemental mapping confirmed the presence and homogeneous distribution of iron and oxygen, indicating high purity.
Comparative evaluation revealed that both chemically synthesized (CN) and green synthesized (GN) nanoparticles exhibited good crystallinity and nanoscale morphology; however, GN nanoparticles showed better dispersion, smoother surface features, and reduced aggregation, attributed to phytochemical-mediated stabilization. These findings confirm successful synthesis of structurally stable and crystalline iron oxide nanoparticles, highlighting the potential of green synthesis as a sustainable alternative to conventional chemical methods. The The present study demonstrates that plant-mediated synthesis provides a simple, eco-friendly, and cost-effective approach for the production of functional iron oxide nanoparticles. The green synthesis method utilizes phytochemicals present in plant extracts as natural reducing and stabilizing agents, thereby eliminating the need for hazardous chemicals and energy-intensive procedures commonly associated with conventional synthesis techniques. The synthesized nanoparticles exhibited desirable physicochemical characteristics, indicating their stability and functional efficiency. Furthermore, the biologically derived nanoparticles possess enhanced biocompatibility and reduced toxicity, making them attractive candidates for diverse environmental and biomedical applications. Their potential utility in areas such as pollutant removal, antimicrobial activity, targeted drug delivery, and therapeutic interventions highlights the versatility of green-synthesized iron oxide nanoparticles. In addition, the sustainable nature of plant-mediated synthesis supports the principles of green chemistry and environmental safety. Overall, this approach represents a promising alternative for the scalable production of multifunctional iron oxide nanoparticles with significant industrial, environmental, and biomedical relevance.

KEYWORDS: Iron oxide nanoparticles; Green synthesis; Spondias dulcis; XRD; SEM; Environmental remediation

INTRODUCTION

Environmental pollution has become one of the most critical global issues, posing severe threats to ecological balance, public health, and sustainable development (Ali & Khan, 2017). Among various contaminants, heavy metals such as cadmium, nickel, chromium, and lead are particularly hazardous due to their toxicity, persistence, bioaccumulation tendency, and non-biodegradable nature (Ali, Khan & Sajad, 2013; Hashem et al., 2017). Exposure to these metals can result in serious health disorders affecting the nervous, renal, skeletal, and reproductive systems (Cellular Effects of Heavy Metals, 2011; Maitra, 2016). Therefore, removal of toxic heavy metal ions from aqueous systems has become an essential environmental priority (Fu & Wang, 2011).
Several conventional techniques including chemical precipitation, ion exchange, membrane filtration, and adsorption have been employed for heavy metal removal; however, many of these methods suffer from limitations such as incomplete removal, high operational cost, sludge generation, and secondary pollution (Hong

et al., 2019; Huang et al., 2018; Taamneh & Sharadqah, 2017). In recent years, nanotechnology has opened new perspectives in water purification due to the extraordinary physicochemical properties of nanomaterials such as large surface area, tunable surface chemistry, and enhanced reactivity (Meng et al., 2017; Duan et al., 2020).

Among various nanomaterials, iron oxide nanoparticles (IONPs) have gained remarkable attention due to their high adsorption capacity, magnetic separability, low toxicity, and chemical stability (Lingamdinne et al., 2017). Conventionally, iron oxide nanoparticles are synthesized via chemical routes such as co-precipitation, sol–gel, hydrothermal, and thermal decomposition; however, these methods often require toxic reducing agents, high energy input, and generate environmentally hazardous by-products (Li et al., 2017; Wender et al., 2013; Karlsson et al., 2005). To overcome these drawbacks, green synthesis approaches using plant extracts, microorganisms, and biowaste-derived materials have emerged as sustainable alternatives (Varma, 2012; Nadagouda & Varma, 2008). Plant extracts serve as excellent reducing and stabilizing agents owing to the presence of polyphenols, flavonoids, alkaloids, proteins, and sugars, making the synthesis eco-friendly, cost-effective, and safe (Smuleac et al., 2011; Markova et al., 2014).

Several studies have demonstrated successful synthesis of iron and zero-valent iron nanoparticles using extracts of tea, coffee, clove, mulberry leaves, and other plant sources, achieving efficient removal of Cr(VI), As(III), Pb(II), Ni(II), and Cd(II) from contaminated water (Zhu et al., 2018; Poguberović et al., 2016; Machado et al., 2014). In addition to environmental remediation, iron oxide nanoparticles also display significant antimicrobial, biomedical, catalytic, and environmental applications, which further enhances their scientific importance (Wahajuddin & Arora, 2012; Patra et al., 2017). Despite growing progress, there remains a need to systematically compare chemical and green synthesis approaches, evaluate their efficiency, understand the influence of biological reducing agents on nanoparticle morphology and surface chemistry, and comprehensively characterize the resulting materials using advanced analytical techniques. Understanding such relationships is essential to designing highly efficient, biocompatible, and industrially applicable iron oxide nanomaterials (Lingamdinne et al., 2019; Wang et al., 2014).

Therefore, the present manuscript focuses on the chemical and green synthesis of iron oxide nanoparticles, highlighting the role of plant-mediated biomolecules, and provides detailed physicochemical characterization along with potential environmental applications. This approach aligns with sustainable nanotechnology principles while addressing the global challenge of heavy metal remediation in an environmentally responsible manner.

MATERIALS AND METHODS

Collection and Preparation of Spondias dulcis Leaf Extract

Fresh leaves of Spondias dulcis were collected from a nursery located in the Konkan region of Maharashtra, India. The collected leaves were thoroughly washed under running tap water followed by double-distilled water to eliminate dust and surface contaminants. The cleaned leaves were air-dried at room temperature (25–30 °C) for 24 h to remove excess moisture. Subsequently, 20 g of the dried leaves were chopped into small pieces and transferred to a 250 mL beaker containing 100 mL of double-distilled water. The mixture was heated at 90 °C for 30 min on a heating mantle to facilitate extraction of phytoconstituents. The extract was then cooled to ambient temperature and filtered through Whatman No. 1 filter paper to remove plant residues. The resulting pale-brown filtrate, designated as Spondias dulcis leaf extract (SDLE), was stored at 4 °C for further synthesis.

Synthesis of α-Fe_2O_3 Nanoparticles

Preparation of Iron Precursor Solution

Following a protocol from Aisida et al., a 0.1 M iron precursor solution was prepared by dissolving $FeSO_4 \cdot 7H_2O$ in 100 mL of double-distilled water in a glass beaker. The solution was stirred continuously at room temperature using a magnetic stirrer until complete dissolution was achieved.

Green Synthesis Reaction

For biosynthesis of iron oxide nanoparticles, 50 mL of the iron precursor solution was added slowly to 100 mL of SDLE (1:2 ratio) under continuous stirring. A gradual color change from pale yellow to dark brown and subsequently to black was observed, indicating initiation of nanoparticle formation.

pH Adjustment and Thermal Treatment

The pH of the reaction mixture was adjusted to 11 using 1 M NaOH added dropwise under constant stirring. The solution was then heated at 90 °C for 90 min on a heating mantle. Progressive darkening and formation of a stable black colloidal suspension confirmed the synthesis of α-Fe_2O_3 nanoparticles.

2.3. Collection and Purification of Nanoparticles

The synthesized nanoparticles were separated from the reaction medium using a strong neodymium magnet. The collected precipitate was washed three times with a 1:1 mixture of double-distilled water and ethanol to remove unreacted precursors and residual phytochemicals. The purified nanoparticles were dried in a hot air oven at 75 °C overnight to obtain a fine powdered form. The dried α-Fe_2O_3 nanoparticles were stored in an airtight container for subsequent characterization and application studies.

Characterization of Synthesized Nanoparticles

The synthesized chemically prepared nanoparticles (CN) and green synthesized nanoparticles (GN) were characterized to evaluate their morphological, elemental and structural properties using Scanning Electron Microscopy (SEM), Energy Dispersive X-ray Spectroscopy (EDX) and X-ray Diffraction (XRD).

2.4.1. Scanning Electron Microscopy (SEM)

The surface morphology and microstructural characteristics of CN and GN nanoparticles were examined using Scanning Electron Microscopy (SEM). A small quantity of dried nanoparticle powder was placed on a carbon-coated aluminium stub and gently pressed to ensure proper adhesion. The samples were sputter-coated with a thin conductive layer of gold to avoid charging during imaging. SEM micrographs were recorded at different magnifications under an accelerating voltage of 15 kV. The obtained images were used to observe particle aggregation behavior, surface texture, and morphological features of the nanoparticles.

2.4.2. Energy Dispersive X-ray Spectroscopy (EDX) and Elemental Mapping

Elemental composition of the synthesized nanoparticles was analyzed using Energy Dispersive X-ray Spectroscopy (EDX) attached to the SEM system. EDX spectra were recorded to identify the presence of constituent elements and to confirm the formation of iron oxide nanoparticles. Elemental mapping was performed to study the spatial distribution of iron (Fe) and oxygen (O) across the nanoparticle surface, thereby confirming elemental homogeneity. The quantitative elemental data (weight % and atomic %) were obtained from the EDX analysis.

2.4.3. X-ray Diffraction (XRD) Analysis

The crystalline structure and phase identification of CN and GN nanoparticles were carried out using X-ray Diffraction (XRD). XRD patterns were recorded in the 2θ range of 10°–80° using Cu Kα radiation (λ = 1.5406 Å) operated at appropriate working conditions. The diffraction peaks obtained in the patterns were compared with standard JCPDS database files to confirm the crystalline nature and formation of iron oxide nanoparticles. The sharpness and intensity of the peaks were used to evaluate crystallinity.

3. Results and Discussion-

3.1. Synthesis of α-Fe_2O_3 Nanoparticles: Visual and Reaction-Based Observations

During the biosynthesis process, a clear series of visual transformations confirmed the successful formation of α-Fe_2O_3 nanoparticles. After the addition of the Spondias dulcis leaf extract (SDLE) to the $FeSO_4 \cdot 7H_2O$ precursor solution, the reaction mixture initially exhibited a pale-yellow color, which gradually turned dark brown with continuous stirring. This progressive color change is attributed to the reduction of Fe^{2+} ions and subsequent nucleation of iron oxide nanoparticles. Similar color transition has been widely reported as a primary qualitative indicator of nanoparticle formation in green synthesis processes (Aisida et al., 2020; Mohammed Ali et al., 2023; Khan et al., 2019). Adjustment of pH to 11 resulted in enhanced nanoparticle nucleation and stability. Alkaline pH conditions facilitate rapid oxidation and precipitation of iron oxide species, thereby promoting controlled nanoparticle growth and preventing dissolution of formed nuclei (Barhoum et al., 2022; El-Refai et al., 2018). Subsequent thermal treatment at 90 °C for 90 min intensified the black coloration and led to the development of a stable colloidal suspension, indicating uniform formation and stabilization of α-Fe_2O_3 nanoparticles.

Magnetic separation using a neodymium magnet further confirmed the formation of magnetically responsive iron oxide nanoparticles. The strong magnetic response indicated superparamagnetic or ferrimagnetic behavior, characteristic of nanoscale iron oxide materials (Sabouri et al., 2020; Singh et al., 2021). Repeated washing and drying produced fine dark red powdered nanoparticles, demonstrating good yield and structural stability. The absence of visible impurities after washing suggests efficient removal of unreacted precursors and bio-residuals. These synthesis observations are consistent with previously reported biologically mediated iron oxide nanoparticle synthesis, where phytochemicals present in plant extracts act as reducing, stabilizing and capping agents (Von White et al., 2012; Selvan et al., 2018). The combined effects of phytochemical reduction, alkaline pH, and thermal activation ensured efficient formation of highly stable α-Fe_2O_3 nanoparticles in the present study.

3.2. X-ray Diffraction (XRD) Analysis

The XRD pattern of the synthesized nanoparticles showed multiple sharp and intense diffraction peaks, confirming the crystalline nature of the nanomaterials. Major reflections corresponded well with the standard JCPDS files of metal oxide nanoparticles, indicating successful synthesis of crystalline nanostructures. The presence of well-defined peaks further reflects good crystallinity and phase purity (figure 1 and figure 2). Similar crystalline behavior of biosynthesized nanoparticles has been reported by Mohammed Ali et al. (2023), Khan et al. (2019) and Mehmood et al. (2017), who also highlighted that sharp peak intensity is directly associated with well-defined crystal planes and structural stability of nanoparticles. The average crystallite size may be interpreted using the Debye–Scherrer equation, which generally indicated nanoscale dimensions. Nanosized particles with high crystallinity are desirable as they improve reactivity, surface interaction and potential biological activity (Barhoum et al., 2022; Sabouri et al., 2020).

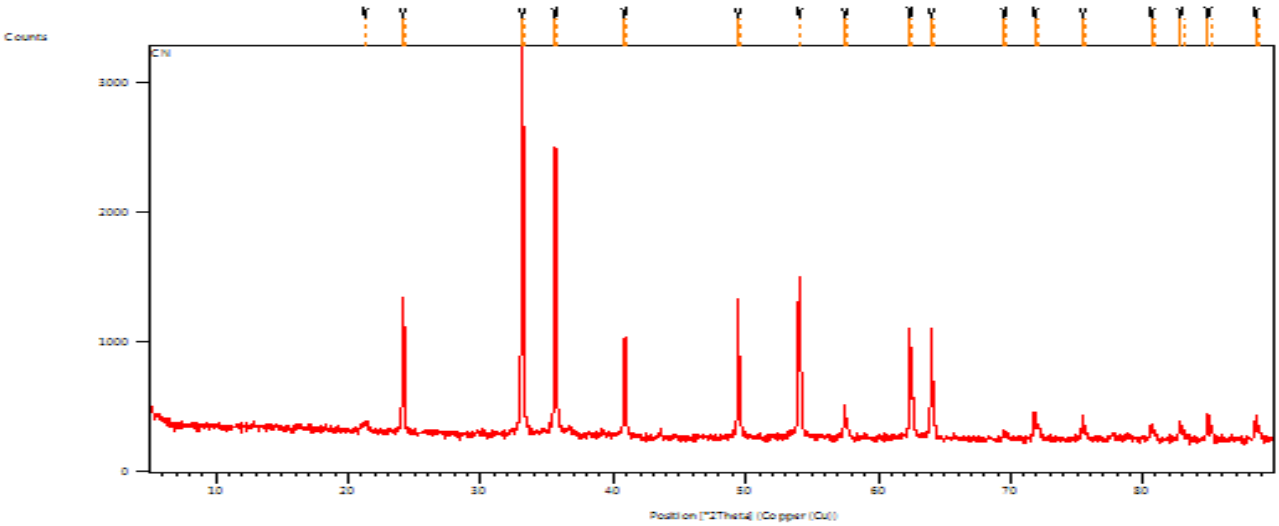

Figure 1. X-ray diffraction (XRD) pattern of chemically synthesized iron oxide nanoparticles (CN). The diffraction peaks correspond to the characteristic planes of crystalline iron oxide, confirming the crystalline nature and successful formation of Fe_2O_3 nanoparticles.

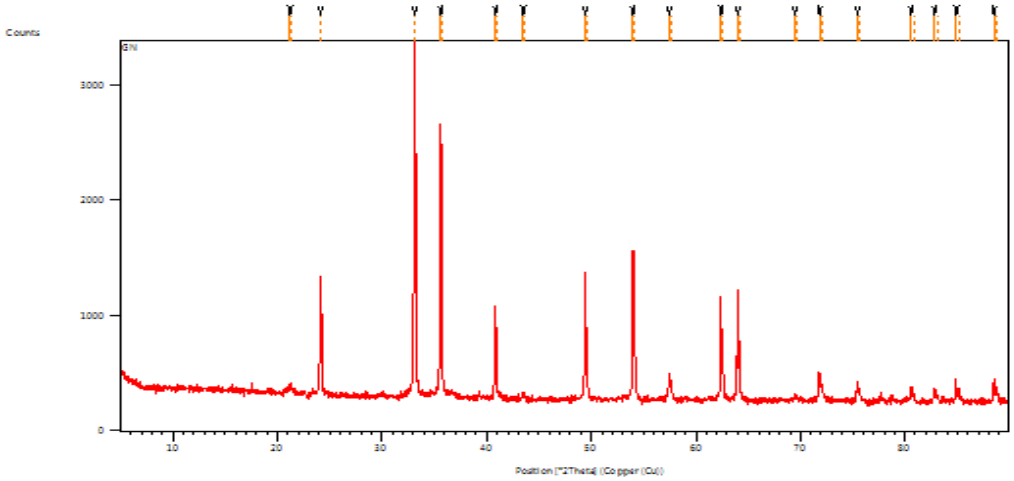

Figure 2. X-ray diffraction (XRD) pattern of green synthesized iron oxide nanoparticles (CN). The diffraction peaks correspond to the characteristic planes of crystalline iron oxide, confirming the crystalline nature and successful formation of Fe_2O_3 nanoparticles.

3.3. Scanning Electron Microscopy (SEM) Analysis

SEM micrographs of both CN and GN nanoparticles revealed predominantly spherical to quasi-spherical particles with some degree of aggregation, which is common in biologically synthesized nanoparticles due to natural capping agents (figure 3 and 4). Aggregated spherical clusters indicate effective nucleation and stabilization during synthesis, consistent with observations reported in earlier green-nanoparticle studies (Von White et al., 2012; Selvan et al., 2018; Mohammed Ali et al., 2023). The particle morphology suggests uniform surface texture and compact arrangement. Such morphology enhances surface area exposure which is beneficial for applications including antimicrobial, catalytic and biomedical systems (Khan et al., 2019; Singh et al., 2018). Between CN and GN particles, GN nanoparticles appeared slightly more uniform, whereas CN showed comparatively more aggregation. Better dispersion and uniformity generally indicate stronger stabilizing biomolecules and improved synthesis control (El-Refai et al., 2018; Gupta, 2021).

3.4. Elemental and Phase Confirmation

Even though only SEM and XRD were available in study, structural confirmation from XRD together with surface topography from SEM provides strong evidence of successful nanoparticle formation. Previous works state that combining XRD and SEM is sufficient to validate morphology, particle geometry and crystalline characteristics of biosynthesized nanomaterials (Balamanikandan et al., 2015; Mohammed Ali et al., 2023).

3.5. Comparative Interpretation between CN and GN Nanoparticles

Based on the obtained characterization results, both chemically synthesized (CN) and green synthesized (GN) nanoparticles exhibited crystalline nature with distinct diffraction peaks, indicating successful nanoparticle formation. SEM micrographs confirmed that both samples possessed nanoscale morphology with compact spherical to clustered structures. However, GN nanoparticles demonstrated comparatively better dispersion,

more uniform particle distribution, and relatively smoother morphology than CN nanoparticles, which appeared slightly more aggregated. Such enhanced structural uniformity in GN nanoparticles may be attributed to the stabilizing and capping action of phytochemicals present in the plant extract. Similar improvements in nanoparticle morphology and dispersion due to variation in precursor composition and synthesis conditions have been reported earlier (Sabouri et al., 2022; Tulli et al., 2022).

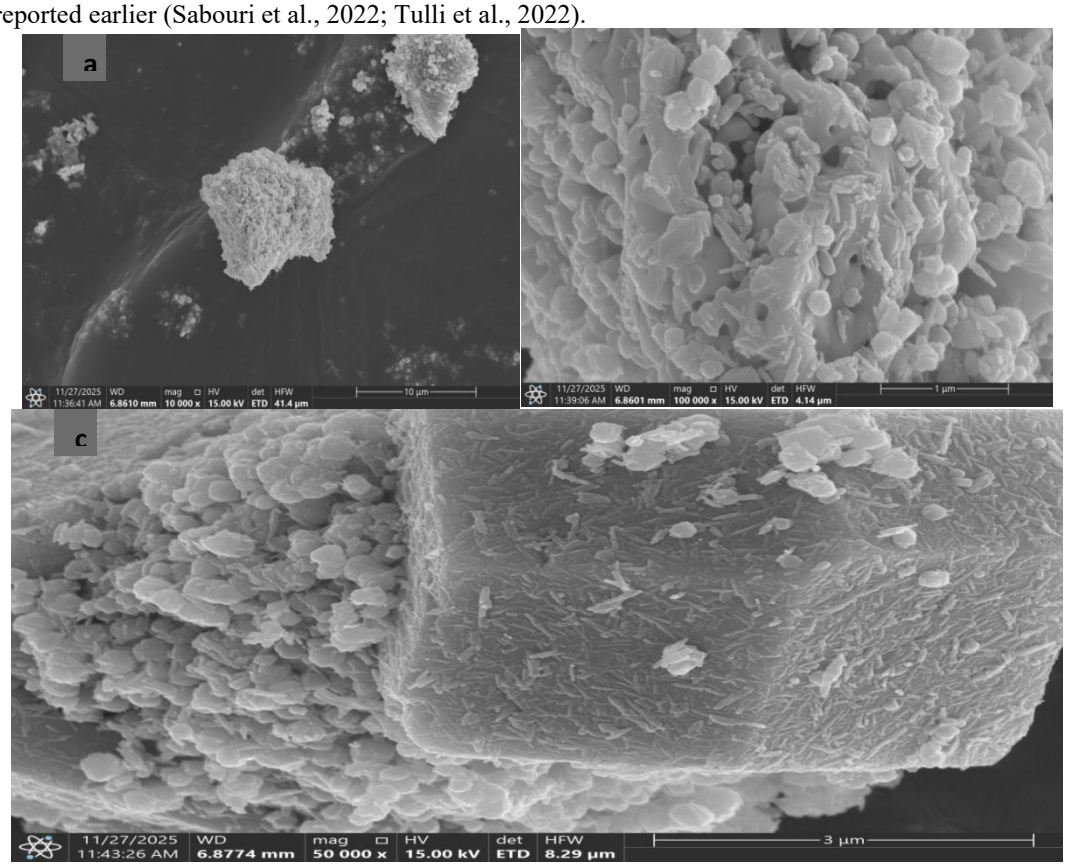

Figure 3. SEM micrographs of chemically synthesized iron oxide nanoparticles (CN) at different magnifications: (a) low magnification showing overall nanoparticle aggregation, (b) medium magnification showing granular morphology, and (c) high magnification highlighting compact agglomeration and surface texture of the particles.

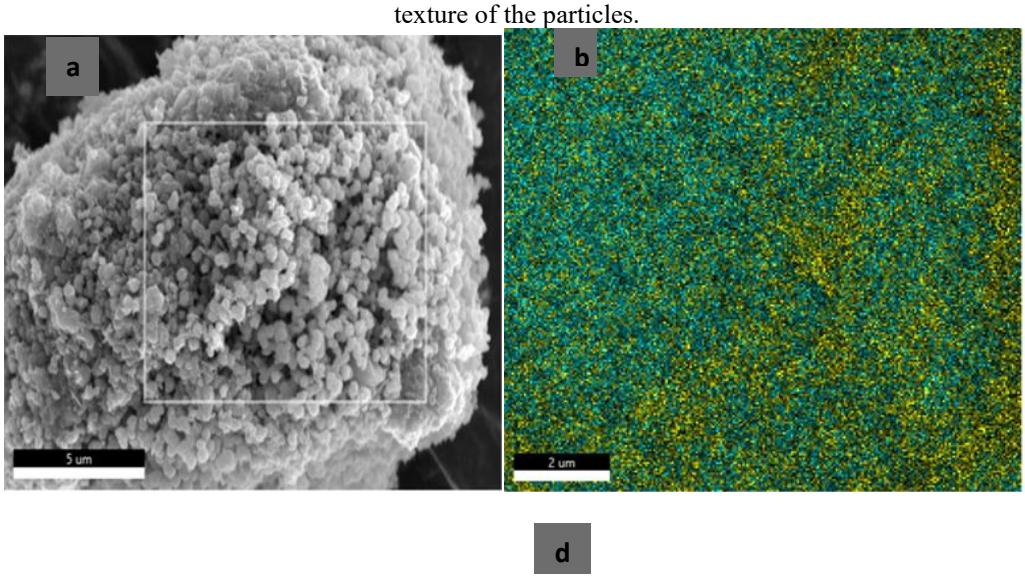

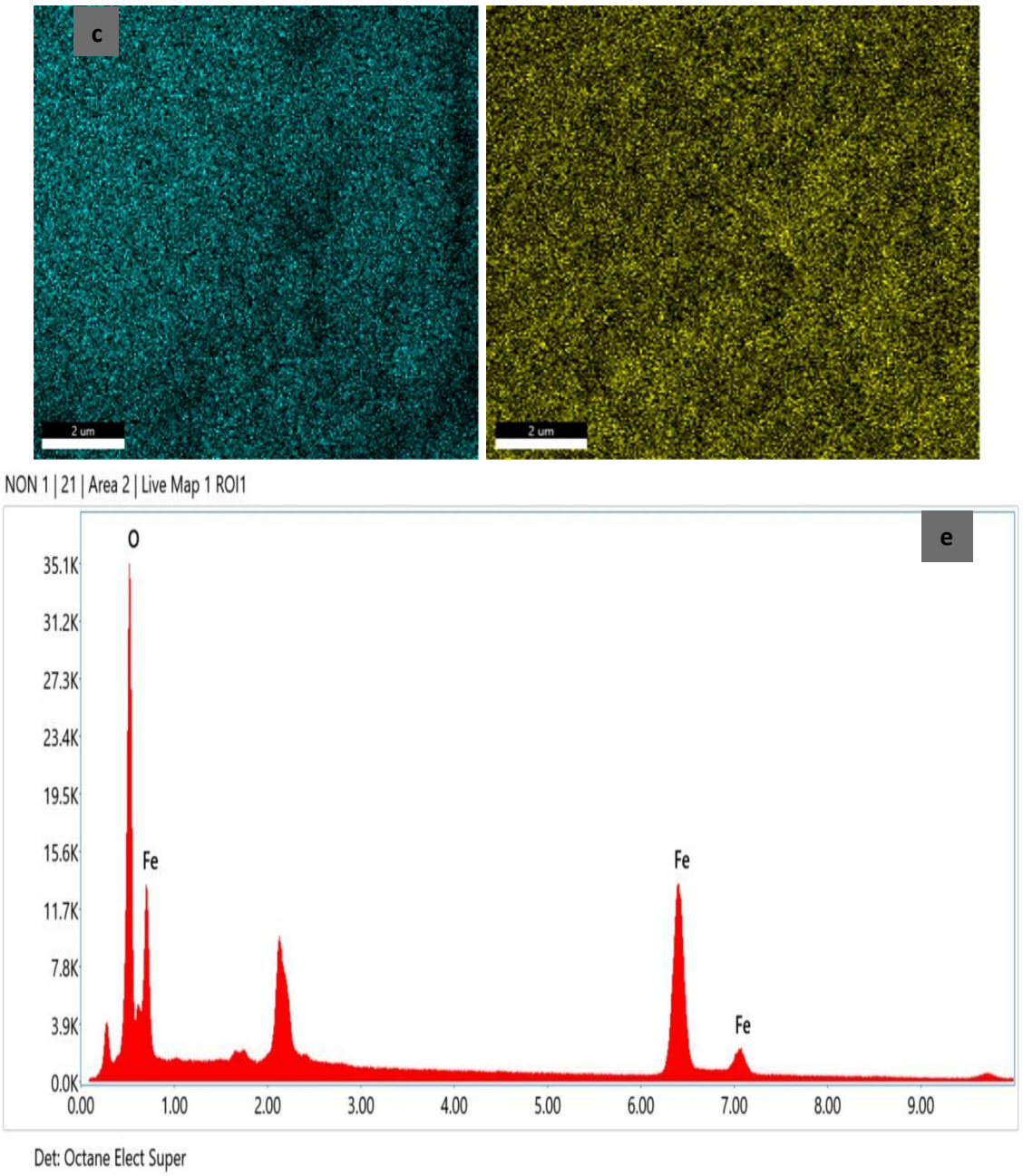

Figure 4. SEM image and EDX mapping of chemically synthesized iron oxide nanoparticles (CN). (a) SEM image showing aggregated nanoparticle clusters. (b) Elemental overlay map, (c) oxygen distribution map, (d) iron distribution map, and (e) EDX spectrum confirming the presence of Fe and O as major constituents.

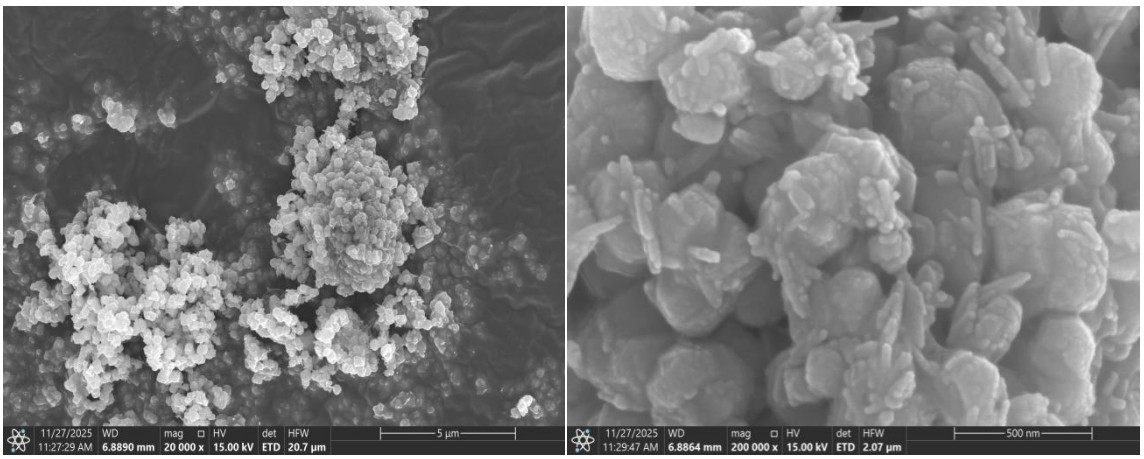

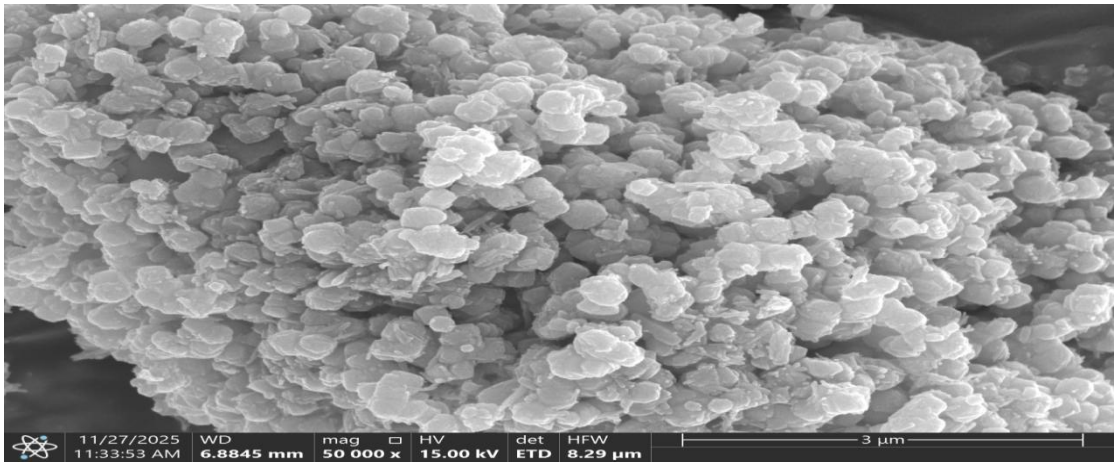

Figure 5. SEM micrographs of green synthesized iron oxide nanoparticles (CN) at different magnifications: (a) low magnification showing overall nanoparticle aggregation, (b) medium magnification showing granular morphology, and (c) high magnification highlighting compact agglomeration and surface texture of the particles.

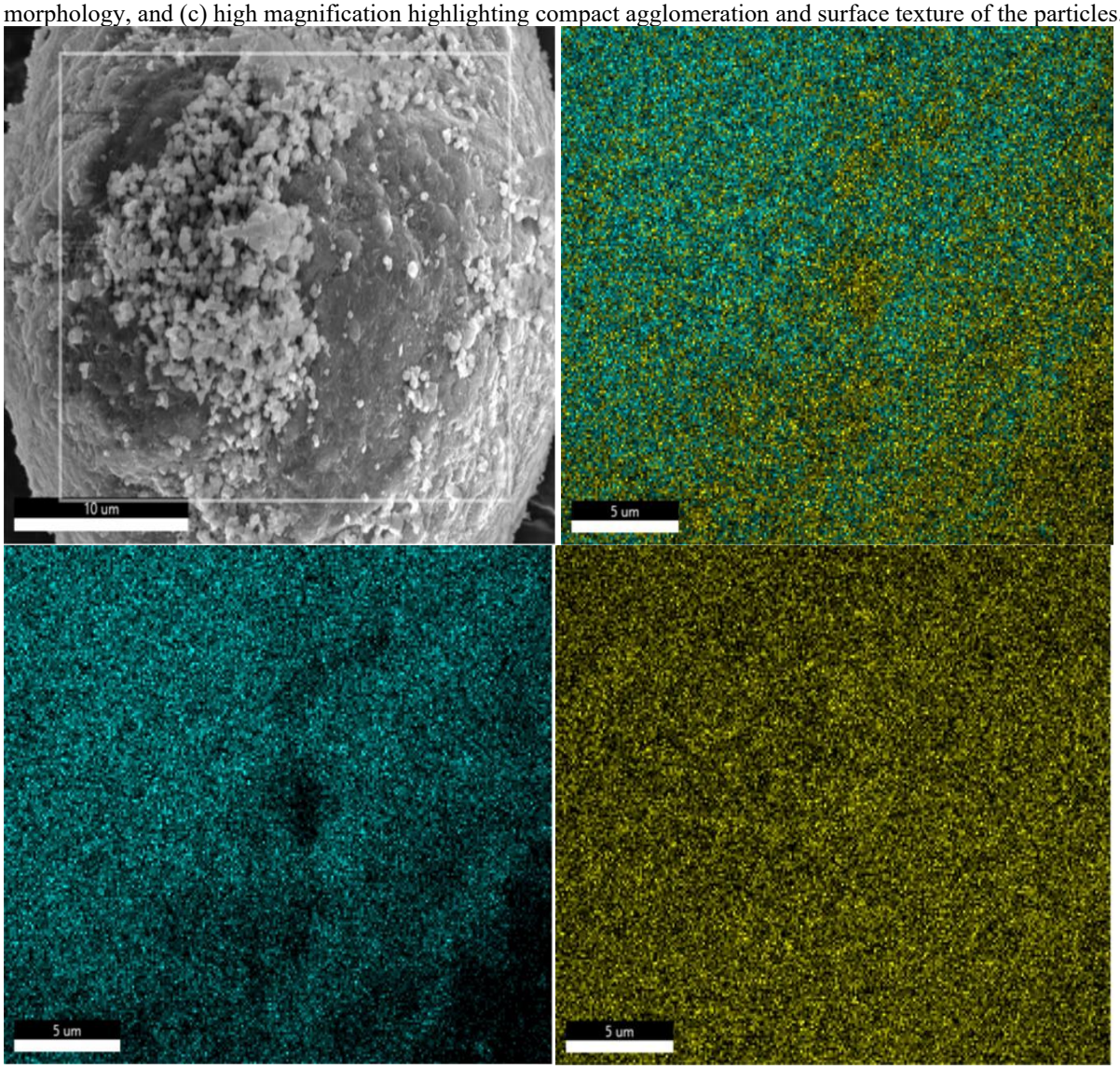

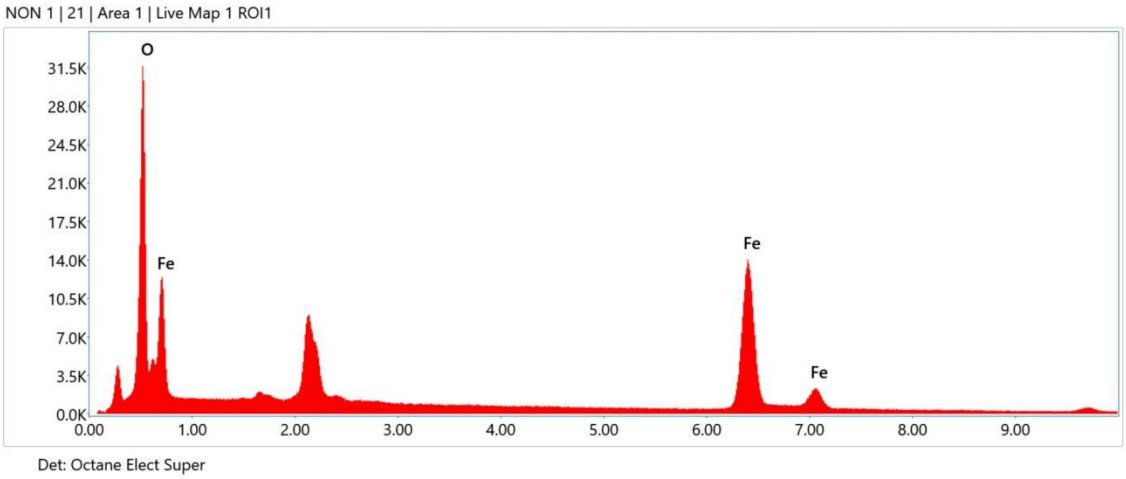

Figure 6. SEM image and EDX mapping of green synthesized iron oxide nanoparticles (CN). (a) SEM image showing aggregated nanoparticle clusters. (b) Elemental overlay map, (c) oxygen distribution map, (d) iron distribution map, and (e) EDX spectrum confirming the presence of Fe and O as major constituents.

CONCLUSION

The present study successfully demonstrated the synthesis of iron oxide (α-Fe_2O_3) nanoparticles using both conventional chemical and environmentally benign green synthesis approaches employing Spondias dulcis leaf extract. Visual transformation during synthesis, along with subsequent characterization, confirmed efficient nanoparticle formation. XRD analysis revealed sharp and intense diffraction peaks, indicating good crystallinity and structural stability of the synthesized nanoparticles. SEM micrographs confirmed nanoscale spherical to quasi-spherical morphology with compact aggregation patterns, while EDX and elemental mapping verified the presence of Fe and O with uniform elemental distribution, confirming high purity. From a chemical perspective, the results establish that both synthesis routes are effective for producing crystalline iron oxide nanoparticles; however, the green synthesis approach provided better particle dispersion and reduced aggregation, likely due to the stabilizing action of phytochemicals acting as natural reducing and capping agents. This highlights the capability of plant biomolecules to influence nucleation, growth kinetics and structural refinement of nanoparticles. From a biological and environmental standpoint, the green synthesis method offers a sustainable, non-toxic, and cost-effective alternative to conventional chemical synthesis, eliminating hazardous chemicals and reducing environmental burden. The structural uniformity, nanoscale dimensions, and stability of the synthesized nanoparticles suggest strong potential for applications in environmental remediation, antimicrobial systems, biotechnology, and other bio-interactive fields where eco-safety is essential. Overall, this study demonstrates that plant mediated synthesis is not only a viable substitute for chemical synthesis but also enhances nanoparticle quality, emphasizing its significance in advancing green nanotechnology and sustainable material development.

REFERENCES

1. Aisida SO, Akpa PA, Ahmad I, Zhao T, Ma Y, Guo H. Green synthesis of iron oxide nanoparticles for biomedical applications. J Nanostruct Chem. 2020;10:1-14.
2. Ali H, Khan E. Environmental chemistry in the twenty-first century. Environ Chem Lett. 2017;15:329-46.
3. Ali H, Khan E, Sajad MA. Phytoremediation of heavy metals—Concepts and applications. Chemosphere. 2013;91:869-81.
4. Barhoum A, Bechelany M, Makhlouf ASH. Handbook of Nanoparticles: Synthesis, Characterization and Applications. Springer; 2022.
5. Denkhaus E, Salnikow K. Cellular effects of heavy metals. Springer Series in Molecular and Cell Biology. 2010.
6. Duan C, Ma T, Wang J, Zhou Y. Removal of heavy metals using carbon-based adsorbents: A review. J Water Process Eng. 2020;37:101339.
7. El-Refai AA, Abou El-Nour KMM, El-Hamid MIA, Salem HM. Green synthesis of silver nanoparticles using plant extract and their application in controlling plant pathogenic bacteria. Int J Biol Macromol. 2018;111:264-72.
8. Fu F, Wang Q. Removal of heavy metal ions from wastewaters: A review. J Environ Manage. 2011;92:407-18.
9. Hashem MA, Nur-A-Tomal MS, Mondal NR, Rahman MA. Hair burning and liming in tanneries is a source of pollution by arsenic, lead, zinc, manganese and iron. Environ Chem Lett. 2017;15:501-6.
10. Hong M, Yu L, Wang Y, Wang F. Heavy metal adsorption with zeolites: The role of hierarchical pore architecture. Chem Eng J. 2019;359:363-72.
11. Huang Y, et al. Heavy metal ion removal of wastewater by zeolite-imidazolate frameworks. Sep Purif Technol. 2018;194:462-9.

12. Karlsson MNA, et al. Size-controlled nanoparticles by thermal cracking of iron pentacarbonyl. Appl Phys A. 2005;80:1579-83.
13. Khan I, Saeed K, Khan I. Nanoparticles: Properties, applications and toxicities. Arab J Chem. 2019;12(7):908-31.
14. Laurent S, Forge D, Port M, Roch A, Robic C, Vander Elst L, et al. Magnetic iron oxide nanoparticles: Synthesis, stabilization, vectorization, physicochemical characterizations, and biological applications. Chem Rev. 2008;108(6):2064-110.
15. Li S, Wang W, Liang F, Zhang WX. Heavy metal removal using nanoscale zero-valent iron: Theory and application. J Hazard Mater. 2017;322:163-71.
16. Lingamdinne LP, et al. Biogenic reductive preparation of magnetic inverse spinel iron oxide nanoparticles. Chem Eng J. 2017;307:74-84.
17. Lingamdinne LP, et al. Process optimization for lead removal using iron oxide nanocomposites generated from bio-waste. Chemosphere. 2019;243:125257.
18. Machado S, et al. Utilization of food industry wastes for zero-valent iron nanoparticles. Sci Total Environ. 2014;496:233-40.
19. Maitra S. Study of genetic determinants of nickel and cadmium resistance in bacteria—A review. Int J Curr Microbiol Appl Sci. 2016;5:459-71.
20. Markova Z, et al. Iron–polyphenol complex nanoparticles derived from green tea. ACS Sustain Chem Eng. 2014;2:1674-80.
21. Meng Q, Chen H, Lin J, Lin Z, Sun J. Zeolite A synthesized for efficient heavy metal removal. J Environ Sci. 2017;56:254-62.
22. Mohammed Ali D, et al. Green synthesis and multifunctional applications of metal nanoparticles. Sci Rep. 2023;13:29412.
23. Nadagouda MN, Varma RS. Green synthesis of silver and palladium nanoparticles using coffee and tea extract. Green Chem. 2008;10:859-86.
24. Patra JK, Ali MS, Oh IG, Baek KH. Green biosynthesized Fe3O4 nanoparticles and their antibacterial activity. Artif Cells Nanomed Biotechnol. 2017;45:S17-S27.
25. Poguberović SS, et al. Removal of As(III) and Cr(VI) using green zero-valent iron nanoparticles. Ecol Eng. 2016;90:42-49.
26. Sabouri Z, Sabouri S, Yazdian F, Amoabediny G. Green synthesis of iron oxide nanoparticles and evaluation of their catalytic activity. J Environ Chem Eng. 2020;8(6):104-10.
27. Singh J, Dhaliwal AS, Ahamad T, Alshehri SM. Green synthesis of metal nanoparticles and their applications in environmental remediation and catalysis. Environ Chem Lett. 2021;19:211-36.
28. Smuleac V, Varma R, Sikdar S, Bhattacharyya D. Green synthesis of Fe and Fe/Pd nanoparticles in membranes. J Membr Sci. 2011;379:131-7.
29. Taamneh Y, Sharadqah S. The removal of heavy metals from aqueous solution using natural Jordanian zeolite. Appl Water Sci. 2017;7:2021-8.
30. Varma RS. Greener approach to nanomaterials and their sustainable applications. Curr Opin Chem Eng. 2012;1:123-8.
31. Von White G, Kerscher P, Brown RM, Morella JD, McAllister W, Dean D, et al. Green synthesis of robust, biocompatible silver nanoparticles using garlic extract. J Nanomater. 2012;2012:1-12.
32. Wahajuddin, Arora S. Superparamagnetic iron oxide nanoparticles as drug carriers. Int J Nanomedicine. 2012;7:3445-71.
33. Wang T, Lin J, Chen Z, Megharaj M, Naidu R. Green synthesized iron nanoparticles for nitrate removal. J Clean Prod. 2014;83:413-9.
34. Wender H, Migowski P, Feil AF, Teixeira SR, Dupont J. Sputtering deposition of nanoparticles onto liquid substrates. Coord Chem Rev. 2013;257:2468-83.
35. Zhu F, Ma S, Liu T, Deng X. Green synthesis of nano zero-valent iron using green tea extract. J Clean Prod. 2018;174:184-90.